

Complete OATP1B1 and OATP1B3 deficiency causes human Rotor syndrome by interrupting conjugated bilirubin reuptake into the liver

Evita van de Steeg,¹ Viktor Stránecký,^{2,3} Hana Hartmannová,^{2,3} Lenka Nosková,³ Martin Hřebíček,³ Els Wagenaar,¹ Anita van Esch,¹ Dirk R. de Waart,⁴ Ronald P.J. Oude Elferink,⁴ Kathryn E. Kenworthy,⁵ Eva Sticová,⁶ Mohammad al-Edreesi,⁷ A.S. Knisely,⁸ Stanislav Kmoch,^{2,3} Milan Jirsa,⁶ and Alfred H. Schinkel¹

¹Division of Molecular Biology, The Netherlands Cancer Institute, Amsterdam, The Netherlands. ²Center for Applied Genomics and

³Institute of Inherited Metabolic Diseases, Charles University of Prague, First Faculty of Medicine, Prague, Czech Republic.

⁴Tytgat Institute for Liver and Intestinal Research, Academic Medical Center, Amsterdam, The Netherlands.

⁵Department of Drug Metabolism and Pharmacokinetics, GlaxoSmithKline, Ware, United Kingdom. ⁶Institute for Clinical and Experimental Medicine, Prague, Czech Republic. ⁷Department of Pediatrics, Saudi Aramco Dhahran Health Centre, Dhahran, Saudi Arabia. ⁸Institute of Liver Studies, King's College Hospital, London, United Kingdom.

Bilirubin, a breakdown product of heme, is normally glucuronidated and excreted by the liver into bile. Failure of this system can lead to a buildup of conjugated bilirubin in the blood, resulting in jaundice. The mechanistic basis of bilirubin excretion and hyperbilirubinemia syndromes is largely understood, but that of Rotor syndrome, an autosomal recessive disorder characterized by conjugated hyperbilirubinemia, coproporphyrinuria, and near-absent hepatic uptake of anionic diagnostics, has remained enigmatic. Here, we analyzed 8 Rotor syndrome families and found that Rotor syndrome was linked to mutations predicted to cause complete and simultaneous deficiencies of the organic anion transporting polypeptides OATP1B1 and OATP1B3. These important detoxification-limiting proteins mediate uptake and clearance of countless drugs and drug conjugates across the sinusoidal hepatocyte membrane. OATP1B1 polymorphisms have previously been linked to drug hypersensitivities. Using mice deficient in *Oatp1a/1b* and in the multispecific sinusoidal export pump *Abcc3*, we found that *Abcc3* secretes bilirubin conjugates into the blood, while *Oatp1a/1b* transporters mediate their hepatic reuptake. Transgenic expression of human OATP1B1 or OATP1B3 restored the function of this detoxification-enhancing liver-blood shuttle in *Oatp1a/1b*-deficient mice. Within liver lobules, this shuttle may allow flexible transfer of bilirubin conjugates (and probably also drug conjugates) formed in upstream hepatocytes to downstream hepatocytes, thereby preventing local saturation of further detoxification processes and hepatocyte toxic injury. Thus, disruption of hepatic reuptake of bilirubin glucuronide due to coexisting OATP1B1 and OATP1B3 deficiencies explains Rotor-type hyperbilirubinemia. Moreover, OATP1B1 and OATP1B3 null mutations may confer substantial drug toxicity risks.

Introduction

Rotor syndrome (RS; OMIM #237450) is a rare, benign hereditary conjugated hyperbilirubinemia, also featuring coproporphyrinuria and strongly reduced liver uptake of many diagnostic compounds, including cholescintigraphic tracers (1–6). RS is an autosomal recessive disorder that clinically resembles another conjugated hyperbilirubinemia, the Dubin-Johnson syndrome (DJS; OMIM #237500) (7, 8). In both RS and DJS, mild jaundice begins shortly after birth or in childhood. There are no signs of hemolysis, and routine hematologic and clinical-biochemistry test results are normal, aside from the primarily conjugated hyperbilirubinemia. RS is, however, distinguishable from DJS by several criteria (1, 2, 9, 10): (a) it lacks the hepatocyte pigment deposits typical of DJS; (b) in

RS, but not DJS, there is delayed plasma clearance of unconjugated bromsulphthalein (BSP), an anionic diagnostic dye, and no conjugated BSP appears in plasma (4); (c) the liver in RS is scarcely visualized on ^{99m}Tc-N[2,6-dimethylphenyl-carbamoylmethyl] iminodiacetic acid (^{99m}Tc-HIDA) cholescintigraphy, with slow liver uptake, persistent visualization of the cardiac blood pool, and prominent kidney excretion (5); and (d) total urinary excretion of coproporphyrins is greatly increased in RS, with coproporphyrin I being the predominant isomer (11).

DJS is caused by mutations affecting ABCC2/MRP2, a canalicular bilirubin glucuronide and xenobiotic export pump, thus disrupting bilirubin glucuronide excretion into bile (7, 8). Excretion of bilirubin glucuronides is then redirected into plasma by the action of ABCC3/MRP3, a homolog of ABCC2 that is present in the sinusoidal membrane and is upregulated in DJS (12, 13). The molecular mechanism of DJS is in line with the generally accepted paradigm of normal hepatic bilirubin excretion, according to which a unidirectional elimination pathway is postulated: first, uptake of unconjugated bilirubin (UCB) from blood into hepatocytes; subse-

Authorship note: Evita van de Steeg and Viktor Stránecký, and Milan Jirsa and Alfred H. Schinkel contributed equally to this work.

Conflict of interest: The research group of Alfred H. Schinkel receives revenues from commercial distribution of some of the mouse strains used in this study.

Citation for this article: *J Clin Invest.* 2012;122(2):519–528. doi:10.1172/JCI59526.

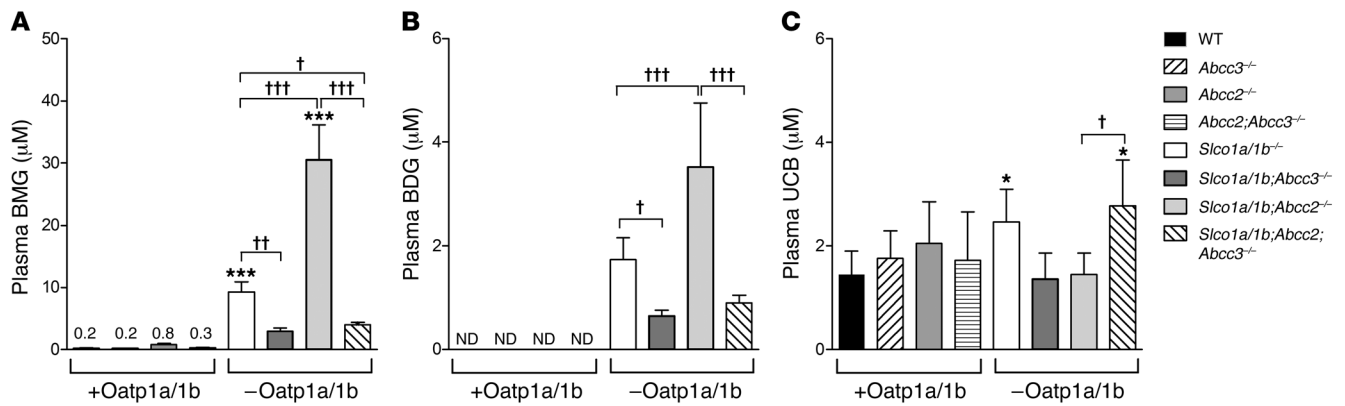


Figure 1

Increased plasma bilirubin glucuronide in *Slco1a/1b*^{-/-} mice is in part dependent on *Abcc3*. (A) BMG, (B) BDG, and (C) UCB levels in plasma of male wild-type, *Abcc3*^{-/-}, *Abcc2*^{-/-}, *Abcc2*^{-/-}*Abcc3*^{-/-}, *Slco1a/1b*^{-/-}, *Slco1a/1b*;*Abcc3*^{-/-}, *Slco1a/1b*;*Abcc2*^{-/-}, and *Slco1a/1b*;*Abcc2*;*Abcc3*^{-/-} mice (*n* = 4–7). +*Oatp1a/1b* denotes strains possessing *Oatp1a/1b* proteins, and –*Oatp1a/1b* denotes strains lacking *Oatp1a/1b* proteins. Data are mean ± SD. **P* < 0.05, ****P* < 0.001 compared with wild-type mice. Bracketed comparisons: †*P* < 0.05, ††*P* < 0.01, †††*P* < 0.001. ND, not detectable; detection limit was 0.1 µM.

quent glucuronidation; and finally, secretion of bilirubin glucuronide into bile via *ABCC2*. Individuals with RS, however, lack *ABCC2* mutations (14), and the mechanistic basis of RS is unknown.

Organic anion transporting polypeptides (OATPs, genes: *SLCOs*) contain 12 plasma membrane-spanning domains and mediate sodium-independent cellular uptake of highly diverse compounds, including bilirubin glucuronide, bile acids, steroid and thyroid hormones, and numerous drugs, toxins, and their conjugates (15, 16). Human OATP1B1 and OATP1B3 localize to the sinusoidal membrane of hepatocytes and mediate the liver uptake of, among other compounds, many drugs (15–19). Various SNPs in *SLCO1B1* cause reduced transport activity and altered plasma and tissue levels of statins, methotrexate, and irinotecan in patients, potentially resulting in life-threatening toxicities (20–24).

In a *Slco1a/1b*^{-/-} mouse model recently generated by our group, the importance of *Oatp1a/1b* proteins in hepatic uptake and clearance of drugs was confirmed, but the mice also displayed marked conjugated hyperbilirubinemia (25). We therefore hypothesized that sinusoidal *Oatps* in the normal, healthy mouse liver function in tandem with the sinusoidal efflux transporter *Abcc3* to mediate substantial hepatic secretion and reuptake of bilirubin glucuronides and other conjugated compounds (25).

Here we describe how a combination of functional studies in mice to address this hypothesis and independent genetic studies in humans has resulted in elucidation of the genetic and mechanistic basis of Rotor syndrome.

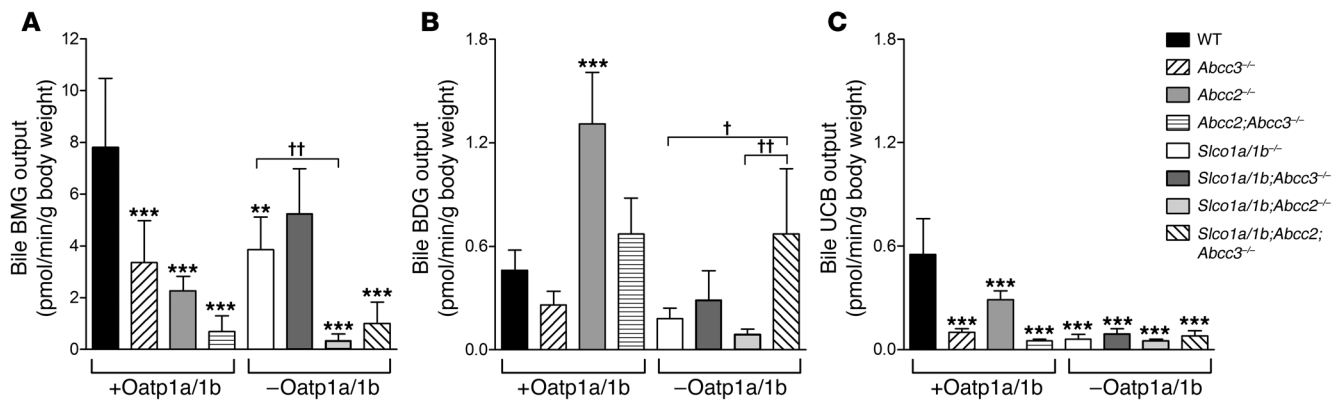
Results

To test our hypothesis regarding the involvement of *Abcc3* in the sinusoidal cycling of bilirubin glucuronides, and to assess a possible interplay with *Abcc2*, we generated *Slco1a/1b*^{-/-}*Abcc3*^{-/-} (*Slco1a/1b*;*Abcc3*^{-/-}), *Slco1a/1b*^{-/-}*Abcc2*^{-/-} (*Slco1a/1b*;*Abcc2*^{-/-}), and *Slco1a/1b*^{-/-}*Abcc2*^{-/-}*Abcc3*^{-/-} (*Slco1a/1b*;*Abcc2*;*Abcc3*^{-/-}) mice by crossbreeding of existing strains. All strains were fertile, with normal life spans and body weights. As previously found for *Abcc2*^{-/-} and *Abcc2*^{-/-}*Abcc3*^{-/-} mice (26, 27), liver weights of *Slco1a/1b*;*Abcc2*^{-/-} and *Slco1a/1b*;*Abcc2*;*Abcc3*^{-/-} mice were significantly increased (~30% and ~50%, respectively) compared with wild-type

mice (data not shown). Quantitative RT-PCR analysis of functionally relevant uptake and efflux transporters in liver, kidney, and intestine of the single and combination knockout strains revealed only some modest expression changes (Supplemental Table 1 and Supplemental Results; supplemental material available online with this article; doi:10.1172/JCI59526DS1). Hepatic UDP-glucuronosyltransferase 1a1 (*Ugt1a1*) expression was not significantly altered in any of the strains.

Importantly, the markedly increased plasma bilirubin mono-glucuronide (BMG) and bilirubin diglucuronide (BDG) levels observed in *Slco1a/1b*^{-/-} mice were substantially reduced in *Slco1a/1b*;*Abcc3*^{-/-} mice, demonstrating that *Abcc3* is necessary for most of this increase (Figure 1, A and B). Plasma BMG levels in *Slco1a/1b*;*Abcc2*^{-/-} mice, even further increased owing to strongly reduced biliary BMG excretion (Figure 2, A and B), were similarly decreased in *Slco1a/1b*;*Abcc2*;*Abcc3*^{-/-} mice (Figure 1, A and B). Thus, *Abcc3* secretes bilirubin glucuronides back into blood, and *Oatp1a/1b* proteins mediate their efficient hepatic reuptake, thereby together establishing a sinusoidal liver-blood shuttling loop. The incomplete reversion of plasma bilirubin glucuronide levels in the *Oatp1a/1b*/*Abcc3*-deficient strains (Figure 1, A and B) suggests that additional sinusoidal exporter(s), e.g., *Abcc4* (28), can partly take over the sinusoidal bilirubin glucuronide extrusion function of *Abcc3*.

The biliary output of bilirubin glucuronides in the single and combination knockout mice showed that, as long as *Oatp1a/1b* was functional, *Abcc3* improved the efficiency of biliary bilirubin glucuronide excretion, even though it transports its substrates initially from liver to blood, not bile (Figure 2, A and B, strains +*Oatp1a/1b*). This suggests that, within liver lobules, the bilirubin glucuronide extruded by *Abcc3* in upstream hepatocytes is efficiently taken up in downstream hepatocytes via *Oatp1a/1b* and then excreted into bile. The resulting relief of possible saturation of (or competition for) biliary excretion in the upstream hepatocytes may explain why the overall biliary excretion is enhanced by this transfer to downstream hepatocytes. However, when *Oatp1a/1b* was absent, *Abcc3* instead decreased biliary bilirubin glucuronide excretion (Figure 2, strains –*Oatp1a/1b*) and

**Figure 2**

In the presence of Oatp1a/1b, but not in its absence, *Abcc3* enhances biliary excretion of bilirubin glucuronides. (A) BMG, (B) BDG, and (C) UCB output in bile of male wild-type, *Abcc3*^{-/-}, *Abcc2*^{-/-}, *Abcc2*^{-/-}*Abcc3*^{-/-}, *Slco1a/1b*^{-/-}, *Slco1a/1b*^{-/-}*Abcc3*^{-/-}, *Slco1a/1b*^{-/-}*Abcc2*^{-/-}, and *Slco1a/1b*^{-/-}*Abcc2*^{-/-}*Abcc3*^{-/-} mice. Bile collected during the first 15 minutes after gall bladder cannulation was analyzed. +Oatp1a/1b denotes strains possessing Oatp1a/1b proteins, and -Oatp1a/1b denotes strains lacking Oatp1a/1b proteins. Data are shown as mean ± SD (*n* = 4–7). ***P* < 0.01, ****P* < 0.001 compared with wild-type mice. Bracketed comparisons: †*P* < 0.05, ††*P* < 0.01.

redirected excretion toward urine via the increased plasma bilirubin glucuronide levels (Supplemental Figure 1). Obviously, in the absence of Oatp1a/1b-mediated hepatic reuptake, *Abcc3* activity can only decrease hepatocyte levels of bilirubin glucuronide in upstream and downstream hepatocytes alike, and will therefore reduce overall biliary excretion. Thus, both components of the *Abcc3* and Oatp1a/1b shuttling loop are necessary to improve hepatobiliary excretion efficiency.

Human hepatocytes express only two OATP1A/1B proteins at the sinusoidal membrane, OATP1B1 and OATP1B3 (15). To test whether these could mediate the identified Oatp1a/1b functions, and in a liver-specific manner, we generated *Slco1a/1b*^{-/-} mice with liver-specific expression of either human OATP1B1 or OATP1B3. Liver-specific expression was obtained using an apoE promoter (29). These strains were viable and fertile, and displayed normal life spans and body weights. Liver levels of transgenic OATP1B1 and OATP1B3 proteins were similar to those seen in pooled human liver samples (data not shown). Both of the transgenic rescue strains displayed a virtually complete reversal of the increases in plasma and urine levels of BMG and BDG seen in *Slco1a/1b*^{-/-} mice (Figure 3, A and B, and Supplemental Figure 2). This indicates that both human OATP1B1 and OATP1B3 effectively reabsorb bilirubin glucuronides from plasma into the liver, in line with their demonstrated *in vitro* role in bilirubin glucuronide uptake (30). The modest (~1.8-fold) increase in plasma UCB in *Slco1a/1b*^{-/-} mice was also reduced in the rescue strains (Figure 3C), suggesting an ancillary role of these proteins in hepatic UCB uptake.

These findings collectively raised the question as to whether humans with a severe deficiency in OATP1B1 and OATP1B3, possibly leading to a conjugated hyperbilirubinemia, might exist. A literature search suggested RS as a candidate inborn metabolic disorder. A search for RS subjects by part of the present group led to collaboration with another team already working on mapping of the RS gene(s).

In an unbiased approach, scanning the whole genome, we mapped the genomic candidate intervals for RS in 11 RS index subjects from 8 different families, 4 Central European (CE1–CE4), 3 Saudi-Arabian (A1–A3), and 1 Filipino (P1) (Figure 4A and Supplemen-

tal Table 2). Homozygosity mapping identified a single genomic region on chromosome 12 for which 8 tested index subjects and no healthy siblings or parents were homozygous (Figure 4B), suggesting inheritance of both alleles from a common ancestor. Three distinct homozygous haplotypes (R1–R3) segregated with RS: R1 in families CE1, CE2, and CE4; R2 in families CE3, A1, A2, and A3; and R3 in family P1 (Figure 4B; for genotyping details, see Methods). Intersection of these haplotypes defined a candidate genomic region spanning the *SLCO1C1*, *SLCO1B3*, *SLCO1B1*, *SLCO1A2*, and *IAPP* genes (Figure 4B). A parallel genome-wide copy number analysis detected a homozygous deletion within the *SLCO1B3* gene in the R1 haplotype and a homozygous approximately 405-kb deletion encompassing *SLCO1B3* and *SLCO1B1* and the *LST-3TM12* pseudogene in the R2 haplotype (Figure 4B and Supplemental Figure 3).

Sequence analysis revealed predictably pathogenic mutations affecting both *SLCO1B3* and *SLCO1B1* in each of the haplotypes (Figure 4, B–D, Table 1, Supplemental Figure 3, and Supplemental Table 3). In the R1 haplotype, a 7.2-kb deletion removes exon 12 of *SLCO1B3*, encoding amino acids 500–560 of OATP1B3 (702 aa long) and introduces a frameshift and premature stop codon, thus removing the C-terminal 3 transmembrane domains. Furthermore, a nonsense mutation in exon 13, c.1738C→T, introduces a premature stop codon (p.R580X) in R1-linked OATP1B1 (691 aa long), removing the C-terminal one-and-a-half transmembrane domains. The 405-kb R2 deletion encompasses exons 3–15 of *SLCO1B3* (sparing only a small N-terminal region) and the whole of *SLCO1B1*, but not *SLCO1A2*. The R3 haplotype harbors a splice donor site mutation, c.1747+1G→A, in intron 13 of *SLCO1B3*. If *SLCO1B3* is still yielding functional mRNA, this would truncate OATP1B3 after amino acid 582, deleting the C-terminal one-and-a-half transmembrane domains. A nonsense mutation, c.757C→T, in exon 8 of R3-linked *SLCO1B1* introduces a premature stop (p.R253X), truncating OATP1B1 before the C-terminal 7 transmembrane domains. All of these mutations would severely disrupt or annihilate proper protein expression and function. Moreover, they all showed consistent autosomal recessive segregation with the RS phenotype in the investigated families (Table 1). No

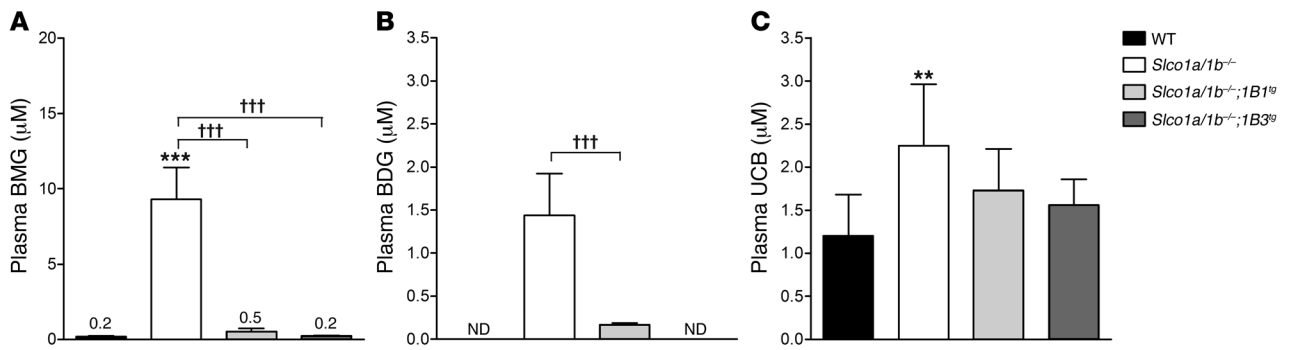


Figure 3 Increased plasma bilirubin glucuronide in *Slco1a/1b*^{-/-} mice is reversed by human OATP1B1 and OATP1B3. (A) BMG, (B) BDG, and (C) UCB levels in plasma of male wild-type and *Slco1a/1b*^{-/-} mice, and of the derived OATP1B1- and OATP1B3-transgenic strains (*Slco1a/1b*^{-/-}; *1B1*^{tg} and *Slco1a/1b*^{-/-}; *1B3*^{tg}, respectively) (n = 5–8). Data are mean ± SD. **P < 0.01, ***P < 0.001 compared with wild-type mice. Bracketed comparisons: †††P < 0.001. Detection limit was 0.1 μM.

SLCO1A2 sequence variation was found in probands representing the 3 haplotypes, rendering involvement of OATP1A2 in RS unlikely. The severity of the identified mutations affecting *SLCO1B3* and *SLCO1B1* and their strict cosegregation with the RS phenotype indicate that RS is caused by co-inherited complete functional deficiencies in both OATP1B3 and OATP1B1.

The severity of the mutations was independently supported by immunohistochemical studies of the sparse RS liver biopsy material available. Given their sparseness, immunostaining of these liver biopsies was performed using one antibody recognizing the N terminus of both OATP1B1 and OATP1B3 (31). This revealed absence of detectable staining in probands representing each haplotype (Figure 5). In controls, basolateral membranes of centrilobular hepatocytes stained crisply, as previously reported (31). Thus, the *SLCO1B1* and *SLCO1B3* mutations in each haplotype result in absence of a detectable signal for OATP1B protein in the liver.

In family A2, a heterozygous splice donor site mutation, c.481+1G→T, in intron 5 of *SLCO1B1* would result in dysfunctional RNA or protein. Its co-occurrence with the 405-kb R2 deletion in two asymptomatic family members (Table 1) indicates that a single functional *SLCO1B3* allele can prevent RS.

A search for copy number variations (CNVs) in existing databases and CNV genotyping of more than 2,300 individuals from various populations (see Supplemental Results) revealed additional heterozygous small and large deletions predicted to disrupt *SLCO1B1* or *SLCO1B3* function, including several approximately 400-kb deletions similar or identical to the R2 haplotype-linked deletion. One individual without jaundice, heterozygous for the R1 haplotype-associated c.1738C→T (p.R580X) mutation in *SLCO1B1*, was also homozygous for the R1 haplotype-associated deletion in *SLCO1B3*. Thus, a single functional *SLCO1B1* allele can also prevent RS. Combined with the findings in family A2 described above, this demonstrates that only a complete deficiency of both alleles of *SLCO1B1* and *SLCO1B3* will result in RS.

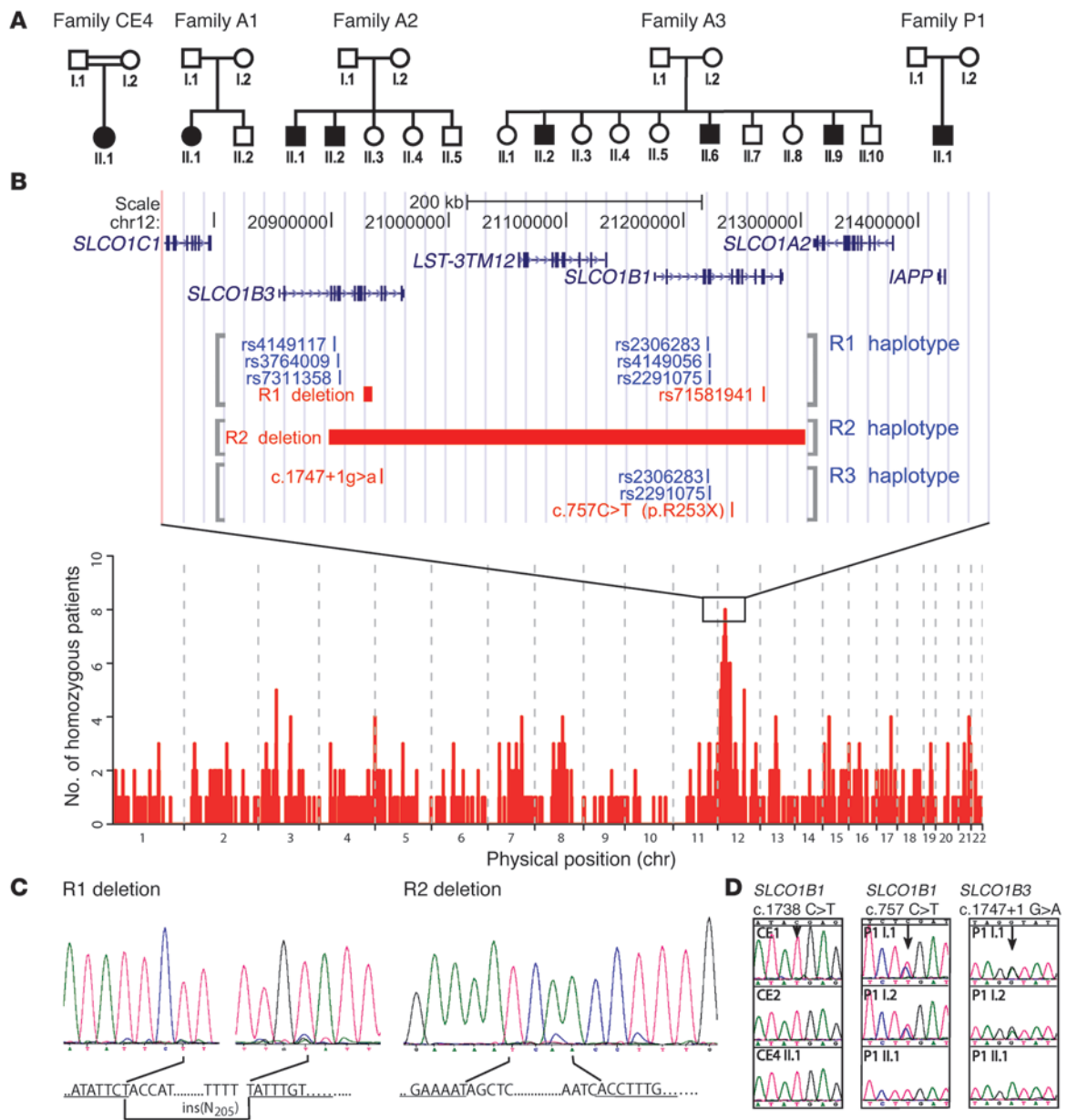
Discussion

We demonstrate here that RS is an obligate two-gene disorder, caused by a complete deficiency of the major hepatic drug uptake transporters OATP1B1 and OATP1B3. We further identified individuals with a complete deficiency of either OATP1B1 or OATP1B3, which was not recognizable by obvious jaundice.

In spite of the documented important functions of especially OATP1B1 in drug detoxification, apparently such deficiencies are compatible with relatively normal life.

Using *Oatp1a/1b*-knockout mice, which can, retrospectively, be considered to be a partial model for RS, we showed that *Abcc3* is an important factor for the RS-like conjugated hyperbilirubinemia. Our data imply that in the normal human liver *ABCC3*, OATP1B1, and OATP1B3 may form a liver-blood shuttling loop for bilirubin glucuronide, similar to that driven by *Oatp1a/1b* and *Abcc3* in the mouse (Figure 6). A substantial fraction of bilirubin conjugated in hepatocytes is secreted back into the blood by *ABCC3* and subsequently reabsorbed in downstream hepatocytes by OATP1B1 and OATP1B3. In RS this reuptake is hampered, causing increased plasma bilirubin glucuronide levels and jaundice. The flexible “hepatocyte hopping” afforded by this loop facilitates efficient detoxification, presumably by circumventing saturation of further detoxification processes in upstream hepatocytes, including excretion into bile. Indeed, we could show that, counterintuitively, but in accordance with the hepatocyte hopping model, loss of *Abcc3* in mice resulted in decreased biliary excretion of bilirubin glucuronide, as long as *Oatp1a/1b* was present (Figure 2). This process likely also enhances hepatic detoxification of numerous drugs and drug conjugates (e.g., glucuronide, sulfate, and glutathione conjugates) transported by OATP1B1/3 and *ABCC3*. Moreover, this principle may also apply to other saturable hepatocyte detoxifying processes, such as phase I and phase II metabolism, as long as the substrate compounds involved are transported by *ABCC3* and OATP1B proteins. Additional sinusoidal efflux and uptake transporters (e.g., *ABCC4*, OATP2B1, NTCP) will further widen the scope of compounds affected by this hepatocyte hopping process. Results obtained with the *Slco1a/1b;Abcc3*-knockout mice indeed show that in addition to *Abcc3* there must be other sinusoidal efflux processes for bilirubin glucuronides. Preventing accumulation of drug glucuronides may be particularly important, since protein adduction by acyl-glucuronides is a well-established cause of drug (hepato)toxicity (32).

One should exercise caution when extrapolating mouse data to humans, and the individual *Oatp1a/1b* proteins are not straightforward orthologs of human OATP1B1 and OATP1B3. However, there is a strong analogy between the bilirubin phenotypes of *Oatp1a/1b*-knockout mice and human Rotor subjects. Moreover, the hepatic transgenic expression of human

**Figure 4**

RS families display deficiencies in *SLCO1B1* and *SLCO1B3*. **(A)** Pedigrees of the investigated families. Black symbols denote RS index subjects. Parents in family CE4 had a documented common ancestor. Families CE1–CE3 (only single individuals analyzed) are not shown. **(B)** Homozygosity regions in 8 RS index subjects and overview of detected mutations and polymorphisms. The genome map shows number and location of overlapping homozygosity regions in RS index subjects, gene content of the top candidate region on chromosome 12, and the genotypes forming all 3 identified RS haplotypes. Mutations crucial for RS are shown in red. chr, chromosome. **(C)** Sequences and electropherograms of the R1 and R2 deletion breakpoints. **(D)** Pathogenic point mutations in R1 and R3 haplotypes. Electropherograms indicate the c.1738C→T (p.R580X) mutation in *SLCO1B1* in probands CE1, CE2, and CE4 II.1 and the c.757C→T (p.R253X) and c.1747+1G→A mutations in *SLCO1B1* and *SLCO1B3*, respectively, in family P1.

OATP1B1 or OATP1B3 resulted in virtually complete rescue of the *Oatp1a/1b*-knockout phenotype for bilirubin handling (Figure 3). This strongly supports that the principles governing bilirubin handling by *Oatp1a/1b* in mouse liver also apply to OATP1B1 and OATP1B3 in human liver.

Analogous to the mouse data for *Oatp1a/1b* (25), the extensive glucuronidation of bilirubin in Rotor subjects suggests that OATP1B1 and/or OATP1B3 are not strictly essential for uptake of UCB into

the liver. Passive transmembrane diffusion is one likely candidate to take over this process, in hepatocytes and probably many other cell types as well (e.g., ref. 33), but we do not exclude that additional uptake transporters (perhaps OATP2B1) can also contribute to UCB uptake. However, OATP1B1 and/or OATP1B3 probably do contribute to hepatic UCB uptake, since in RS subjects a significant increase in plasma UCB is usually observed and reduced clearance of UCB has been reported (34, 35). Moreover, polymorphisms in *SLCO1B1*



Table 1
Mutations in *SLCO1B* genes detected in RS subjects and their family members

Subject	Family status	Haplotype R1-linked mutations		Haplotype R2-linked mutations		Haplotype R3-linked mutations	
		<i>SLCO1B3</i> 7.2-kb deletion	<i>SLCO1B1</i> c.1738C→T (p.R580X) rs71581941	<i>SLCO1B</i> locus 405-kb deletion	<i>SLCO1B1</i> c.481+1G→T splice site mutation	<i>SLCO1B3</i> c.1747+1G→A splice site mutation	<i>SLCO1B1</i> c.757C→T (p.R253X)
CE1	Proband	del/del	T/T				
CE2	Proband	del/del	T/T				
CE4 I.1	Father	del/WT	T/C				
CE4 I.2	Mother	del/WT	T/C				
CE4 II.1	Proband	del/del	T/T				
CE3	Proband			del/del	-/-		
A1 I.1	Father			del/WT	-/G		
A1 I.2	Mother			del/WT	-/G		
A1 II.1	Proband			del/del	-/-		
A1 II.2	Brother			WT/WT	G/G		
A2 I.1	Father			del/WT	-/G		
A2 I.2	Mother			del/WT	-/T		
A2 II.1	Brother			del/del	-/-		
A2 II.2	Proband			del/del	-/-		
A2 II.3	Sister			del/WT	-/T		
A2 II.4	Sister			del/WT	-/G		
A2 II.5	Brother			WT/WT	G/T		
A3 I.1	Father			del/WT	-/G		
A3 I.2	Mother			del/WT	-/G		
A3 II.1	Sister			WT/WT	G/G		
A3 II.2	Proband			del/del	-/-		
A3 II.3	Sister			del/WT	-/G		
A3 II.4	Sister			del/WT	-/G		
A3 II.5	Sister			del/WT	-/G		
A3 II.6	Brother			del/del	-/-		
A3 II.7	Brother			del/WT	-/G		
A3 II.8	Sister			del/WT	-/G		
A3 II.9	Brother			del/del	-/-		
A3 II.10	Brother			WT/WT	G/G		
P1 I.1	Father					G/A	C/T
P1 I.2	Mother					G/A	C/T
P1 II.1	Proband					A/A	T/T

Boldface indicates index subjects with RS ($n = 11$; 8 probands, 3 affected siblings); 405-kb deletion (assembly NCBI36/hg18) — g.(20898911)_ (21303509)del(CA)ins; 7.2-kb deletion (assembly NCBI36/hg18) — g.(20927077)_(20934292)del(N205)ins. WT, wild-type sequence, i.e., sequence from which all exons of *SLCO1B1* and *SLCO1B3* could be amplified. Genotypes for all empty entries were wild-type in sequence and/or heterozygous or homozygous for the large haplotype R2-linked deletion as predicted.

and *SLCO1B3* have been associated with increased serum UCB levels (36, 37). There was also a significant, nearly 2-fold increase in plasma UCB in the *Sco1a/1b*^{-/-} mice, and this was partially reversed by both human OATP1B1 and OATP1B3 expression (Figure 3C).

It should be noted that UGT1A1-mediated glucuronidation may also occur in extrahepatic tissues, for instance, colon (38), and we cannot exclude that some of the bilirubin glucuronide observed in RS plasma has resulted from such extrahepatic glucuronidation, possibly enhanced by the increased plasma UCB levels. It seems unlikely, however, that all bilirubin glucuronide in RS subjects would derive from extrahepatic glucuronidation. This would require a complete block of hepatic UCB uptake (due to the OATP1B1 and OATP1B3 deficiency), but at the same time require efficient uptake of UCB into UGT1A1-containing extrahepatic cells (e.g., colonocytes) that do not normally express OATP1B1 and OATP1B3, and certainly not in Rotor subjects. If UCB transmembrane diffusion can do this efficiently, it is hard to see why this would not

mediate substantial uptake into the liver as well. Only if hepatic diffusion uptake is negligible (which seems physically unlikely) and an unknown efficient UCB uptake system would function in colonocytes (and not in liver), could one envisage such a situation. On balance, this seems rather implausible.

Elucidation of OATP1B1 and OATP1B3 deficiency as the cause of RS can also readily explain the other diagnostic traits of the disorder. Absence of OATP1B1/3-mediated liver uptake would cause the decreased plasma clearance of anionic diagnostic dyes such as indocyanine green and BSP, an excellent substrate of OATP1B1 and OATP1B3 (15), and the greatly reduced or delayed visualization of the liver by anionic cholescintigraphic radiotracers such as ^{99m}Tc-HIDA and ^{99m}Tc-mebrofenin (5, 6). ^{99m}Tc-mebrofenin, for instance, is efficiently transported by both OATP1B1 and OATP1B3 (39).

The markedly increased urinary excretion of coproporphyrins, and the increased preponderance of isomer I over III in urine of RS subjects, could be simply explained by reduced (re)uptake of

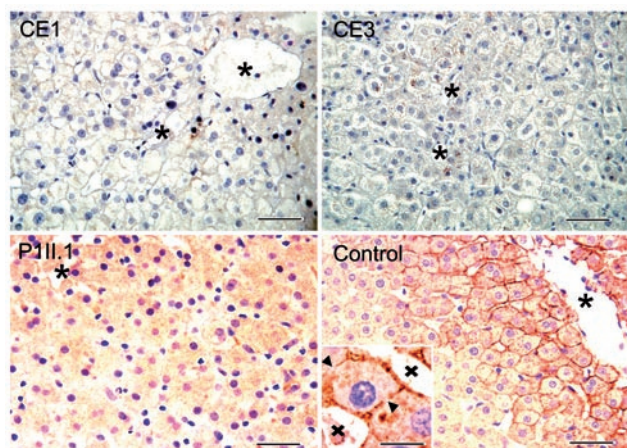


Figure 5

Liver expression of OATP1B proteins in RS subjects and control. With an anti-OATP1B/3 antibody, basolateral membrane immunostaining of hepatocytes in centrilobular areas was intense in control. Asterisks indicate central veins, arrowheads bile canaliculi, and crosses sinusoids. OATP1B proteins were not detectable in RS subjects CE1 (haplotype R1), CE3 (haplotype R2), and P11.1 (haplotype R3). Scale bars: 25 μm (original magnification of CE1 and CE3, $\times 400$; original magnification of P11.1 and control, $\times 200$); inset: 5 μm (original magnification, $\times 1,000$).

these compounds into the liver, partly shifting the excretion route from hepatobiliary/fecal to urinary, especially for isomer I. Coproporphyrin I and III thus most likely are transported substrates of OATP1B1 and OATP1B3. Indeed, interaction of several porphyrins with OATP1B1 has recently been demonstrated (40).

Phenotypic abnormalities in RS subjects are surprisingly moderate. Perhaps OATP1B1 and OATP1B3 functions are partly taken over by other sinusoidal uptake transporters, such as OATP2B1. Nevertheless, since even reduced-activity OATP1B1 polymorphisms can result in life-threatening drug toxicities (20–24, 41, 42), such risks are likely increased substantially in RS subjects. Their evident jaundice, however, may have been a warning sign for physicians to prescribe drugs with caution.

The obligatory deficiency in two different, medium-sized genes explains the rarity of RS, with a roughly estimated frequency of about 1 in 10^6 , although it might be several-fold lower or higher in different populations. Complete deficiency of either OATP1B1 or OATP1B3 alone will occur much more frequently but will not cause jaundice. For instance, the p.R580X mutation in OATP1B1 occurred at an allele frequency of 0.008 (3 of 354) in a Japanese population (43), suggesting that about 1 in 14,000 individuals in this population would be homozygous for this full-deficiency mutant. Such individuals might demonstrate idiosyncratic hypersensitivity to OATP1B1 substrate drugs, including statins or irinotecan. Similarly, in the present study we identified a non-jaundiced individual homozygously deficient for *SLCO1B3* in our CNV screening of approximately 2,300 individuals, in line with a non-negligible incidence of fully OATP1B3-deficient individuals.

Some drugs, such as high-dose cyclosporine A, can transiently increase plasma levels of conjugated bilirubin without evoking other markers for liver damage (44, 45). Until now, such increases were thought to be primarily mediated by inhibition of ABCC2 as the main biliary excretion factor for bilirubin glucuronide.

However, given the insights from the present study, direct inhibition of OATP1B1 and/or OATP1B3 by the applied drug may be an additional or even the main cause of such drug-induced conjugated hyperbilirubinemia. This might for instance apply to cyclosporine A, rifampin, rifamycin SV, or other drugs that are established inhibitors of OATP1B proteins (23). Moreover, heterozygous carriers of the various full-deficiency mutations in OATP1B1/3 might be more susceptible to such inhibitory effects. This also applies to drug-drug interactions mediated through OATP1B1/3 inhibition.

The molecular mechanism we identified in RS may also underlie a similar disorder called hepatic uptake and storage syndrome, or conjugated hyperbilirubinemia type III (OMIM $\%237550$) (46). This hypothesis can now be tested by mutational analysis of OATP1B1 and OATP1B3 in the only reported family to date. Furthermore, a mutant strain of Southdown sheep has also been described as displaying a similar hepatic uptake and storage syndrome (46), and it would not surprise us if these animals would likewise have a deficiency of one or more hepatic sinusoidal OATPs. The observation that mutant Southdown sheep, like the *Slco1a1b*^{-/-} mice (25), also display strongly reduced clearance of (unconjugated) cholic acid, but not of (conjugated) taurocholic acid (47), further supports this idea.

Collectively, our findings explain the genetic and molecular basis of RS. The demonstration of an Abcc3-, OATP1B1-, and OATP1B3-driven detoxification-enhancing liver-blood shuttling loop in mice and, by implication, most likely also in humans challenges the view of one-way excretion from blood through liver to bile of bilirubin and drugs detoxified by conjugation. Furthermore, the identified full-deficiency alleles of *SLCO1B1* and *SLCO1B3* may contribute to various “idiosyncratic” drug hypersensitivities.

Methods

Mouse strains and conditions. Mice were housed and handled according to institutional guidelines complying with Dutch legislation. *Slco1a1b*^{-/-}, *Abcc2*^{-/-}, *Abcc3*^{-/-}, and *Abcc2*^{-/-}*Abcc3*^{-/-} mice have been described (25–27, 48). Human OATP1B1 transgenic mice have been described (29), and human OATP1B3 transgenic mice were generated in an analogous manner, using an apoE promoter to obtain liver-specific expression of the transgene. Each transgene was crossed back into an *Slco1a1b*^{-/-} background to obtain the corresponding humanized rescue strains. Routine mouse conditions and analyses of mouse samples are described in Supplemental Methods.

Western blot analysis. Isolation of crude membrane fractions from mouse liver, kidney, and small intestine and Western blotting were as described previously (29). For detection of Abcc2 and Abcc3 primary antibodies, M₂III-5 (dilution 1:1,000) and M₃-18 (dilution 1:25) were used, respectively. For detection of transgenic OATP1B1 and OATP1B3 in mouse liver, the rabbit polyclonal antibodies ESL and SKT, provided by D. Keppler (Deutsches Krebsforschungszentrum, Heidelberg, Germany) were used (17, 18).

RNA isolation, cDNA synthesis, and RT-PCR. RNA isolation from mouse liver, kidney, and small intestine and subsequent cDNA synthesis and RT-PCR were as described previously (49). Specific primers (QIAGEN) were used to detect expression levels of *Slco1a1*, *Slco1a4*, *Slco1a6*, *Slco1b2*, *Slco2b1*, *Slc10a1*, *Slc10a2*, *Abcc2*–4, *Abcb1a*, *Abcb1b*, *Abcb11*, *Abcg2*, *Osta*, *Ostb*, and *Ugt1a1*.

Analysis of bilirubin in mouse plasma, bile, and urine. Gallbladder cannulations and collection of bile and urine in male mice of the various strains ($n = 4$ –7) as well as bilirubin detection were as described (25, 50, 51). For details, see Supplemental Methods.

RS families. We examined 11 RS index subjects (8 probands, 3 siblings of probands) of 8 families and 21 clinically healthy members of 5 of these 8 families. Family members of 3 probands (CE1–CE3) were not available.

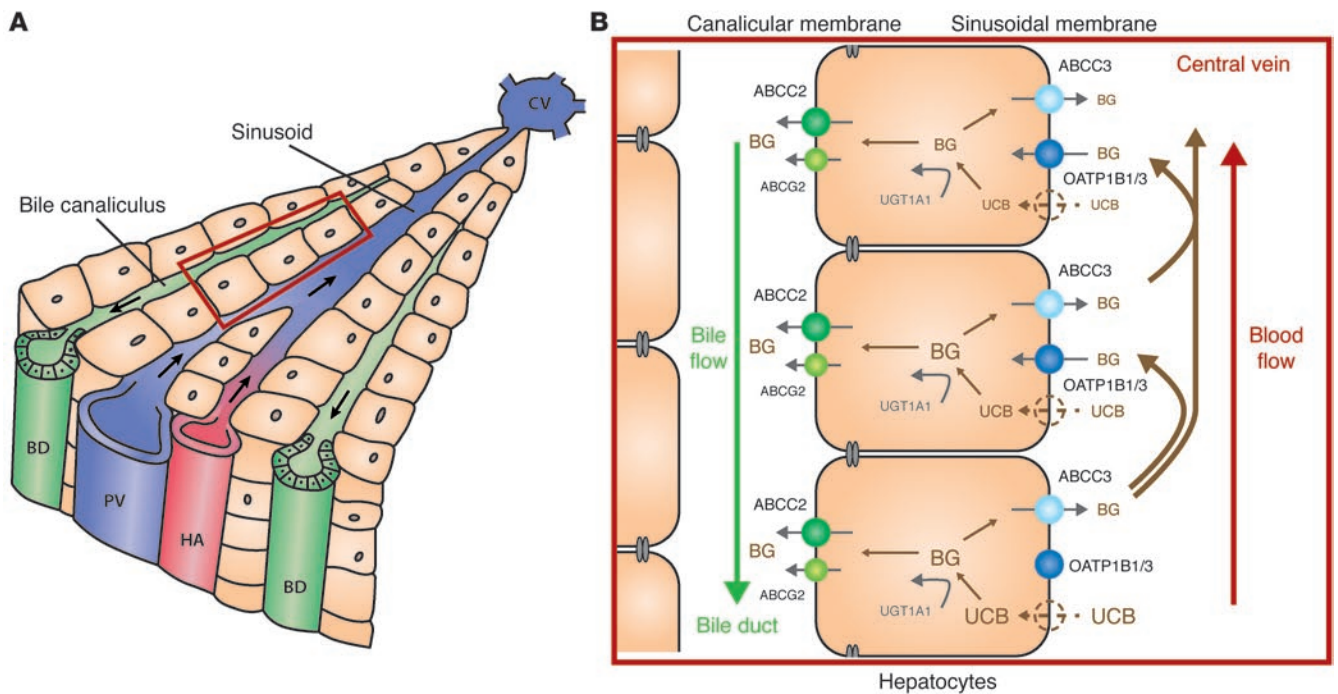


Figure 6 Hepatocyte hopping distributes the biliary excretion load of bilirubin glucuronides across the liver lobule. **(A)** Schematic of liver lobule. Hepatocytes are organized around portal tracts, with branches of the portal vein (PV), hepatic artery (HA), and bile ducts (BD). The PV and HA deliver nutrient- and oxygen-rich blood, respectively, which flows through the sinusoids toward the central vein (CV). Basolateral (sinusoidal) membranes of hepatocytes are flushed with perisinusoidal plasma. Bile flows in the opposite direction toward bile ducts through canaliculi lined by canalicular membranes of hepatocytes. **(B)** Hepatocyte hopping cycle. UCB enters the hepatocytes via passive diffusion and/or transporters, which may include OATP1B1 and/or OATP1B3 in non-Rotor subjects. Conjugation with glucuronic acid by UGT1A1 to bilirubin glucuronides (BG) takes place in endoplasmic reticulum. BG is secreted into bile mainly by ABCC2. ABCG2 also can contribute to this process. Even under physiological conditions, a substantial fraction of the intracellular BG is rerouted by ABCC3 to the blood, from which it can be taken up by downstream hepatocytes via OATP1B1/3 transporters. This flexible off-loading of BG to downstream hepatocytes prevents saturation of biliary excretion capacity in upstream hepatocytes. Relative type sizes of UCB and BG represent local concentrations. Schematic modified, with permission, from ref. 54.

Families CE1–CE4 are of mixed Central European descent by family report. Three families (A1–A3) are Saudi Arabs, and one family (P1) is from the Philippines. Central European families were ascertained at the Institute for Clinical and Experimental Medicine, Prague, and Saudi Arab and Filipino families at the Saudi Aramco Dhahran Health Center. Medical histories were obtained by referring consultants. Subjects CE1 and CE2 were reported as case 1 and case 2, respectively (14).

ABCC2 mutation screening. ABCC2 mutation screening was performed in 8 probands representing all studied families as described previously (14).

Genotyping. Genotyping was performed using Affymetrix GeneChip Mapping 6.0 Arrays (Affymetrix) according to the manufacturer’s protocol. Raw feature intensities were extracted from Affymetrix GeneChip Scanner 3000 7G images using GeneChip Control Console Software 2.01. Individual SNP calls were generated using Affymetrix Genotyping Console Software 3.02. Details of the experiment and individual genotyping data are available at the GEO repository (<http://www.ncbi.nlm.nih.gov/geo>) under accession number GSE33733.

Multipoint nonparametric and parametric linkage analysis. Multipoint nonparametric and parametric linkage analysis along with determination of the most likely haplotypes was performed with version 1.1.2 of Merlin software (52). Parametric linkage was carried out assuming an autosomal recessive mode of inheritance with a 1.00 constant, age-independent penetrance, 0.00 phenocopy rate, and 0.0001 frequency of disease allele. Results

were visualized in version 1.032 of HaploPainter software (53) and in version 2.9.2 of R-project statistical software (<http://www.r-project.org/>).

Homozygosity mapping. Extended homozygosity regions were identified in Affymetrix Genotyping Console Software version 3.02 using the algorithm comparing values from the user’s sample set and SNP-specific distributions derived from a reference set of 200 ethnically diverse individuals. Distribution of extended homozygosity regions in affected and healthy individuals was analyzed and visualized using custom R-script.

Copy number changes. Copy number changes were identified in Affymetrix Genotyping Console Software version 3.02. Data from both SNP and copy number probes were used to identify copy number aberrations compared with built-in reference. Only regions larger than 10 kb containing at least 5 probes were reported.

Quantitative PCR. Quantitative PCR was carried out in duplicate on a LightCycler 480 System (Roche Applied Science). Data were analyzed by LightCycler 480 Software, release 1.5.0. Absolute quantification was used to determine copy number status of a given fragment in analyzed samples. Genomic positions of the analyzed fragments and control genes, corresponding primer sequences, and Universal ProbeLibrary probes used for amplification and quantitation are provided in Supplemental Table 4.

Mutation analysis. Long-range PCR products encompassing the genomic regions of deletion breakpoint boundaries were gel-purified and sequenced using a primer walking approach. DNA sequencing of PCR products and



genomic fragments covering 1 kb of the promoter regions and all of the exons, with their corresponding exon-intron boundaries, of *SLCO1B1*, *SLCO1B3*, and *SLCO1A2* was performed. For details, see Supplemental Methods. Confirmation and segregation of both identified copy number changes and missense mutations in the families, as well as frequency of the mutations in a control population of mixed European descent, were assessed by PCR, PCR-RFLP, and direct sequencing of corresponding genomic DNA fragments. For primer sequences, see Supplemental Table 4.

Histology and immunohistochemistry. Archival liver biopsy specimens were available from 5 unrelated RS index subjects (probands, families CE1, CE2, CE3, and P1; brother [A3 II.9] of proband from family A3). Sections of paraffin-embedded material (formalin or Carnoy solution fixative; 4–6 μ m thick) were routinely stained with hematoxylin and eosin and periodic acid-Schiff techniques. For OATP1B1, OATP1B3, and ABCC2 immunostaining, routine techniques were applied (see Supplemental Methods). OATP1B1 and OATP1B3 detection was performed with a primary mouse anti-OATP1B antibody (clone mMDQ, GeneTex; recognizing the N terminus of both OATP1B1 and OATP1B3), 1:100 dilution, overnight at 4°C (31).

Statistics. One-way ANOVA followed by Tukey's multiple comparison test was used to assess statistical significance of differences between data sets. Results are presented as mean \pm SD. Differences were considered statistically significant when *P* was less than 0.05.

Study approval. All mouse studies were ethically reviewed and carried out in accordance with European directive 86/609/EEC and Dutch legislation and the GlaxoSmithKline policy on the Care, Welfare and Treatment of Laboratory Animals. Experiments were approved by the Animal Experimentation Committee (DEC) of the Netherlands Cancer Institute. Invest-

igations involving humans were approved by the Institutional Review Boards of the Institute for Clinical and Experimental Medicine, Prague, Czech Republic, and the Saudi Aramco Dhahran Health Centre, with written informed consent received from participants or their guardians, and conducted according to Declaration of Helsinki principles.

Acknowledgments

The human study was supported in part by the Ministry of Education of the Czech Republic (projects MSM0021620806 and 1M6837805002) and by the Institute for Clinical and Experimental Medicine (MZO 00023001). The mouse work was supported in part by grant S2918 from GlaxoSmithKline and grant NKI 2007-3764 from the Dutch Cancer Society. The authors thank L. Budišová and M. Boučková for technical assistance and L. Vítek, M. Mikulecký, J. Horák, and A. Šuláková for referring patients CE1–CE4.

Received for publication June 16, 2011, and accepted in revised form November 30, 2011.

Address correspondence to: Alfred H. Schinkel, Division of Molecular Biology, The Netherlands Cancer Institute, Plesmanlaan 121, 1066 CX Amsterdam, The Netherlands. Phone: 31.20.5122046; Fax: 31.20.6961383; E-mail: a.schinkel@nki.nl. Or to: Milan Jirsa, Department of Experimental Medicine, Institute for Clinical and Experimental Medicine, Vídenská 1958/9, 140 00 Prague 4 – Krč, Czech Republic. Phone: 420.261362773; Fax: 420.241721666; E-mail: miji@ikem.cz.

1. Chowdhury JR, Chowdhury NR, Jansen PLM. Bilirubin metabolism and its disorders. In: Boyer TD, Wright TL, Manns MP, Zakim D, eds. *Zakim and Boyer's Hepatology. A Textbook of Liver Diseases*. Vol. 2. Philadelphia, Pennsylvania, USA: Saunders Elsevier; 2006:1449–1474.
2. Chowdhury JR, Wolkoff AW, Chowdhury NR, Arias IM. Hereditary jaundice and disorders of bilirubin metabolism. In: Scriver CR, Beaudet AL, Sly WS, Valle D, eds. *The Metabolic and Molecular Bases of Inherited Disease*. Vol. 2. New York, New York, USA: McGraw Hill; 2001:3063–3101.
3. Rotor AB, Manahan L, Florentin A. Familial nonhemolytic jaundice with direct van den Bergh reaction. *Acta Med Phil*. 1948;5:37–49.
4. Wolpert E, Pascasio FM, Wolkoff AW, Arias IM. Abnormal sulfobromophthalein metabolism in Rotor's syndrome and obligate heterozygotes. *N Engl J Med*. 1977;296(19):1099–1101.
5. Bar-Meir S, Baron J, Seligson U, Gottesfeld F, Levy R, Gilat T. 99mTc-HIDA cholescintigraphy in Dubin-Johnson and Rotor syndromes. *Radiology*. 1982; 142(3):743–746.
6. LeBouthillier G, Morais J, Picard M, Picard D, Chartrand R, Pommier G. Scintigraphic aspect of Rotor's disease with Technetium-99m-mebrofenin. *J Nucl Med*. 1992;33(8):1550–1551.
7. Kartenbeck J, Leuschner U, Mayer R, Keppler D. Absence of the canalicular isoform of the MRP gene-encoded conjugate export pump from the hepatocytes in Dubin-Johnson syndrome. *Hepatology*. 1996;23(5):1061–1066.
8. Paulusma CC, et al. A mutation in the human canalicular multispecific organic anion transporter gene causes the Dubin-Johnson syndrome. *Hepatology*. 1997;25(6):1539–1542.
9. Nowicki MJ, Poley JR. The hereditary hyperbilirubinemia. *Baillieres Clin Gastroenterol*. 1998; 12(2):355–367.
10. Strassburg CP. Hyperbilirubinemia syndromes (Gilbert-Meulengracht, Crigler-Najjar, Dubin-Johnson, and Rotor syndrome). *Best Pract Res Clin Gastroenterol*. 2010;24(5):555–571.
11. Wolkoff AW, Wolpert E, Pascasio FN, Arias IM. Rotor's syndrome. A distinct inheritable pathophysiological entity. *Am J Med*. 1976;60(2):173–179.
12. König J, Rost D, Cui Y, Keppler D. Characterization of the human multidrug resistance protein isoform MRP3 localized to the basolateral hepatocyte membrane. *Hepatology*. 1999;29(4):1156–1163.
13. Lee YM, et al. Identification and functional characterization of the natural variant MRP3-Arg1297His of human multidrug resistance protein 3 (MRP3/ABCC3). *Pharmacogenetics*. 2004;14(4):213–223.
14. Hrebicek M, et al. Rotor-type hyperbilirubinemia has no defect in the canalicular bilirubin export pump. *Liver Int*. 2007;27(4):485–491.
15. Hagenbuch B, Gui C. Xenobiotic transporters of the human organic anion transporting polypeptide (OATP) family. *Xenobiotica*. 2008;38(7–8):778–801.
16. Hagenbuch B, Meier PJ. Organic anion transporting polypeptides of the OATP/SLC21 family: phylogenetic classification as OATP/SLCO superfamily, new nomenclature and molecular/functional properties. *Pflügers Arch*. 2004;447(5):653–665.
17. König J, Cui Y, Nies AT, Keppler D. A novel human organic anion transporting polypeptide localized to the basolateral hepatocyte membrane. *Am J Physiol Gastrointest Liver Physiol*. 2000;278(1):G156–G164.
18. König J, Cui Y, Nies AT, Keppler D. Localization and genomic organization of a new hepatocellular organic anion transporting polypeptide. *J Biol Chem*. 2000;275(30):23161–23168.
19. Abe T, et al. LST-2, a human liver-specific organic anion transporter, determines methotrexate sensitivity in gastrointestinal cancers. *Gastroenterology*. 2001;120(7):1689–1699.
20. Takane H, et al. Life-threatening toxicities in a patient with UGT1A1*6/*28 and SLCO1B1*15/*15 genotypes after irinotecan-based chemotherapy. *Cancer Chemother Pharmacol*. 2009; 63(6):1165–1169.
21. Link E, et al. SLCO1B1 variants and statin-induced myopathy—a genomewide study. *N Engl J Med*. 2008; 359(8):789–799.
22. Treviño LR, et al. Germline genetic variation in an organic anion transporter polypeptide associated with methotrexate pharmacokinetics and clinical effects. *J Clin Oncol*. 2009;27(35):5972–5978.
23. Kalliokoski A, Niemi M. Impact of OATP transporters on pharmacokinetics. *Br J Pharmacol*. 2009; 158(3):693–705.
24. König J, Seithel A, Gradhand U, Fromm MF. Pharmacogenomics of human OATP transporters. *Naunyn-Schmiedeberg's Arch Pharmacol*. 2006; 372(6):432–443.
25. Van de Steeg E, et al. Organic anion transporting polypeptide 1a/1b-knockout mice provide insights into hepatic handling of bilirubin, bile acids and drugs. *J Clin Invest*. 2010;120(8):2942–2952.
26. Vlaming ML, et al. Carcinogen and anticancer drug transport by Mrp2 in vivo: studies using Mrp2 (Abcc2) knockout mice. *J Pharmacol Exp Ther*. 2006; 318(1):319–327.
27. Vlaming ML, et al. Impact of Abcc2 (Mrp2) and Abcc3 (Mrp3) on the in vivo elimination of methotrexate and its main toxic metabolite 7-hydroxymethotrexate. *Clin Cancer Res*. 2008;14(24):8152–8160.
28. Rius M, Nies AT, Hummel-Eisenbeis J, Jedlitschky G, Keppler D. Cotransport of reduced glutathione with bile salts by MRP4 (ABCC4) localized to the basolateral hepatocyte membrane. *Hepatology*. 2003; 38(2):374–384.
29. Van de Steeg E, et al. Methotrexate pharmacokinetics in transgenic mice with liver-specific expression of human OATP1B1 (SLCO1B1). *Drug Metab Dispos*. 2009;37(1):1–5.
30. Cui Y, König J, Leier I, Buchholz U, Keppler D. Hepatic uptake of bilirubin and its conjugates by the human organic anion transporter SLC21A6. *J Biol Chem*. 2001;276(13):9626–9630.
31. Cui Y, et al. Detection of the human organic anion transporters SLC21A6 (OATP2) and SLC21A8 (OATP8) in liver and hepatocellular carcinoma. *Lab Invest*. 2003;83(4):527–538.
32. Zhou S, Chan E, Duan W, Huang M, Chen YZ.



- Drug bioactivation, covalent binding to target proteins and toxicity relevance. *Drug Metab Rev.* 2005; 37(1):41–213.
33. Zucker SD, Goessling W, Hoppin AG. Unconjugated bilirubin exhibits spontaneous diffusion through model lipid bilayers and native hepatocyte membranes. *J Biol Chem.* 1999;274(16):10852–10862.
34. Kawasaki H, Kimura N, Irisa T, Hirayama C. Dye clearance studies in Rotor's syndrome. *Am J Gastroenterol.* 1979;71(4):380–388.
35. Fedeli G, et al. Impaired clearance of cholephilic anions in Rotor syndrome. *Z Gastroenterol.* 1983; 21(5):228–233.
36. Zhang W, et al. OATP1B1 polymorphism is a major determinant of serum bilirubin level but not associated with rifampicin-mediated bilirubin elevation. *Clin Exp Pharmacol Physiol.* 2007;34(12):1240–1244.
37. Sanna S, et al. Common variants in the SLCO1B3 locus are associated with bilirubin levels and unconjugated hyperbilirubinemia. *Hum Mol Genet.* 2009; 18(14):2711–2718.
38. Strassburg CP, Manns MP, Tukey RH. Expression of the UDP-glucuronosyltransferase 1A locus in human colon. Identification and characterization of the novel extrahepatic UGT1A8. *J Biol Chem.* 1998; 273(15):8719–8726.
39. Ghibellini G, Leslie EM, Pollack GM, Brouwer KL. Use of tc-99m mebrofenin as a clinical probe to assess altered hepatobiliary transport: integration of in vitro, pharmacokinetic modeling, and simulation studies. *Pharm Res.* 2008;25(8):1851–1860.
40. Campbell SD, Lau WF, Xu JJ. Interaction of porphyrins with human organic anion transporting polypeptide 1B1. *Chem Biol Interact.* 2009;182(1):45–51.
41. Morimoto K, Oishi T, Ueda S, Ueda M, Hosokawa M, Chiba K. A novel variant allele of OATP-C (SLCO1B1) found in a Japanese patient with pravastatin-induced myopathy. *Drug Metab Pharmacokinet.* 2004;19(6):453–455.
42. Tirona RG, Kim RB. Pharmacogenomics of organic anion-transporting polypeptides (OATP). *Adv Drug Deliv Rev.* 2002;54(10):1343–1352.
43. Kim SR, et al. Genetic variations and frequencies of major haplotypes in SLCO1B1 encoding the transporter OATP1B1 in Japanese subjects: SLCO1B1*17 is more prevalent than *15. *Drug Metab Pharmacokinet.* 2007;22(6):456–461.
44. Yahanda AM, et al. Phase I trial of etoposide with cyclosporine as a modulator of multidrug resistance. *J Clin Oncol.* 1992;10(10):1624–1634.
45. List AF, et al. Phase I/II trial of cyclosporine as a chemotherapy-resistance modifier in acute leukemia. *J Clin Oncol.* 1993;11(9):1652–1660.
46. Dhumeaux D, Berthelot P. Chronic hyperbilirubinemia associated with hepatic uptake and storage impairment. A new syndrome resembling that of mutant southdown sheep. *Gastroenterology.* 1975; 69(4):988–993.
47. Engelking LR, Gronwall R. Bile acid clearance in sheep with hereditary hyperbilirubinemia. *Am J Vet Res.* 1979;40(9):1277–1280.
48. Zelcer N, et al. Mice lacking Mrp3 (Abcc3) have normal bile salt transport, but altered hepatic transport of endogenous glucuronides. *J Hepatol.* 2006; 44(4):768–775.
49. Van Waterschoot RA, et al. Midazolam metabolism in cytochrome P450 3A knockout mice can be attributed to up-regulated CYP2C enzymes. *Mol Pharmacol.* 2008;73(3):1029–1036.
50. Van Herwaarden AE, et al. The breast cancer resistance protein (Bcrp1/Abcg2) restricts exposure to the dietary carcinogen 2-amino-1-methyl-6-phenylimidazo[4,5-b]pyridine. *Cancer Res.* 2003; 63(19):6447–6452.
51. Spivak W, Carey MC. Reverse-phase h.p.l.c. separation, quantification and preparation of bilirubin and its conjugates from native bile. Quantitative analysis of the intact tetrapyrroles based on h.p.l.c. of their ethyl anthranilate azo derivatives. *Biochem J.* 1985;225(3):787–805.
52. Abecasis GR, Cherny SS, Cookson WO, Cardon LR. Merlin — rapid analysis of dense genetic maps using sparse gene flow trees. *Nat Genet.* 2002;30(1):97–101.
53. Thiele H, Nurnberg P. HaploPainter: a tool for drawing pedigrees with complex haplotypes. *Bioinformatics.* 2005;21(8):1730–1732.
54. Van de Steeg E, Iusuf D, Schinkel AH. Physiological and pharmacological functions of OATP1A/1B transporters: insights from knockout and transgenic mice. In: Van de Steeg E. *Physiological and pharmacological functions of OATP1A/1B transporters. PhD thesis, University of Utrecht.* Enschede, the Netherlands: Gildeprint drukkerijen; 2010:9–37.